Sub-T_g relaxation times of the α process in metallic glasses

Chaoren Liu[a], Eloi Pineda[b], Daniel Crespo[a], Jichao Qiao[c], Zach Evenson[d], Beatrice Ruta[e,f]

[a] Departament de Física, Universitat Politècnica Catalunya - BarcelonaTech, EETAC, Esteve Terradas 5, 08860 Castelldefels, Spain.
eloi.pineda@upc.edu

[b] Departament de Física, Universitat Politècnica Catalunya - BarcelonaTech, ESAB, Esteve Terradas 8, 08860 Castelldefels, Spain.
chaorenliu@gmail.com / daniel.crespo@upc.edu

[c] School of Mechanics, Civil Engineering and Architecture, Northwestern Polytechnical University, Xi'an 710072, P. R. China

[d] Heinz Maier-Leibnitz Zentrum (MLZ) and Physik Department, Technische Universität München, Lichtenbergstrasse 1, 85748 Garching, Germany.

[e] Institut Lumière Matière, UMR5306 Université Lyon 1- CNRS, Université de Lyon, 69622 Villeurbanne Cedex, France
beatrice.ruta@univ-lyon1.fr

[f] ESRF – The European Synchrotron, CS 40220, 38043 Grenoble Cedex 9, France.

[*]Corresponding author:
Eloi Pineda
eloi.pineda@upc.edu
Tel. (34) 935 521 141

Abstract

The current view of structural relaxation in metallic glasses assumes the presence of primary and secondary processes with different activation energies. While the faster, secondary process can be well characterized in the out-of-equilibrium state below the glass transition temperature T_g, the experimental direct determination of the primary process in this temperature region is more difficult due to the long relaxation times. In this work, we merge new and literature data to analyze the temperature behavior of the primary relaxation

time below T_g as observed by mechanical spectroscopy and stress relaxation of metallic glasses of different fragility. We compare these results with the microscopic structural relaxation times previously measured with X-ray photon correlation spectroscopy. The coincidence between the macroscopic and microscopic relaxation times allows us to discuss the underlying mechanisms responsible of primary relaxation over different length scales, as well as to propose an overall picture of the primary relaxation behavior in the glassy regime near T_g.

Keywords: relaxation, metallic glasses, mechanical spectroscopy, XPCS, beta relaxation, alpha relaxation, glass transition.

Introduction

A detailed knowledge of the relaxation behavior of metallic glasses is crucial for gaining understanding of some key properties of these materials, such as glass-forming-ability, shape formability, mechanical response and thermal stability. The current understanding of relaxation dynamics of metallic glasses is based on the presence of a secondary or β relaxation, also termed Johari-Goldstein (JG) or 'slow' β relaxation in order to avoid confusion with the fast β processes also found in liquid dynamics [1]. This JG or β relaxation is thought to be the precursor of the primary or α relaxation [2,3]. From a macroscopic point of view, the α process is associated with the transition from an elastic (solid) to a viscous (liquid) response under the application of an external force. When the force is applied during an extended period of time shorter than the α relaxation time, τ_α, the system behaves as an elastic medium, for longer times it relaxes as a viscous fluid. The β relaxation is currently viewed as a reversible or anelastic-like process, preceding

irreversible or liquid-like local movements, whose volume fraction increases with increasing temperature, finally leading to a global viscous response near the glass transition temperature T_g [4].

Above T_g, glass-forming systems are in internal equilibrium. In this regime, the relaxation dynamics, along with all other intrinsic properties, is not dependent on the previous temperature and pressure conditions and is usually probed by mechanical spectroscopy or viscosity measurements [5–7]. The fragility parameter *m* [8] is used to characterize the temperature dependence of the α relaxation time $\tau_\alpha(T)$ in this region. The apparent local activation energy of the liquid near T_g is related to fragility *via* $E_\alpha^{liq} = mRT_g \ln 10$, where *R* is the gas constant.

Below T_g, glasses are arrested in out-of-equilibrium configurations. In this regime, physical aging and rejuvenation may be induced by the ambient conditions or by thermal and mechanical treatments [9–12]. Through physical aging and rejuvenation, the glass changes from one so-called isoconfigurational state to another; in a first order approach, the particular glass configuration can be described by a fictive temperature T_f [13]. We will define here the range of temperatures below, but not far from, T_g as the sub-T_g region. In this temperature range the β process shows short relaxation times, of the order of seconds or less and can be probed experimentally by conventional mechanical spectroscopy or calorimetric techniques [14,15]. In metallic glasses, the activation energy of the secondary process generally follows an overall $E_\beta \approx 26RT_g$ empirical correlation [3]. The activation of shear transformation zones (STZs) also shows similar energy barriers as reviewed in ref. [16]. On the other hand, the α process involves long times and the presence of *in situ*

physical aging complicates the determination of $\tau_\alpha(T)$ of an isoconfigurational glass. The order of magnitude of the aging time τ_{aging} is similar to τ_α and it is therefore difficult to avoid a simultaneous change of the glassy configuration during the required long experimental probes [17].

In this work, we compile and analyze some previous results of measurements of τ_α both above T_g in the equilibrated liquid and in the sub-T_g region. Together with some new stress relaxation results, they give us a panorama picture of the primary relaxation of isoconfigurational metallic glasses in the sub-T_g region. Finally, we discuss the implications of the presented results on the current microscopic and Potential Energy Landscape (PEL) views of α and β processes [4,18].

Experimental

Metallic glass ribbons with chemical compositions (at. %) of $Mg_{65}Cu_{25}Y_{10}$, $Zr_{46}Cu_{46}Al_8$, $Pd_{42.5}Ni_{7.5}Cu_{30}P_{20}$ and $Pd_{43}Ni_{10}Cu_{27}P_{20}$ were produced by melt spinning. All the samples were characterized by X-ray Diffraction (XRD) with a Bruker D8 Advance apparatus and by Differential Scanning Calorimetric analysis (DSC) with NETZSCH 404 F3 and Perkin Elmer DSC-7 instruments. Dynamic Mechanical Analysis (DMA) and static relaxation tests were performed in a TA Q800 apparatus. The DMA measurements were performed at different frequencies, from 0.01 to 100 Hz, and constant heating rates of 0.5-2 K min^{-1}. Static stress-relaxation tests were performed on $Zr_{46}Cu_{46}Al_8$ and $Pd_{42.5}Ni_{7.5}Cu_{30}P_{20}$ applying an 'instantaneous' deformation, typically 10 μm on a 10 mm piece of ribbon, and monitoring the time evolution of the stress under isothermal conditions. The stress evolution, $\sigma(t)$, was followed at each temperature step during 30 min in $Pd_{42.5}Ni_{7.5}Cu_{30}P_{20}$

and 60 min in $Zr_{46}Cu_{46}Al_8$. From DMA and static stress relaxation curves, the relaxation times and the shape parameters of the relaxation functions were obtained by non-linear fitting of the models discussed below. The fittings were performed minimizing the least-squares error weighting each data point by the experimental error. The associated standard errors of the parameter estimates are depicted in Figures 1, 3 and 4. Elongation viscosity measurements were performed on $Pd_{42.5}Ni_{7.5}Cu_{30}P_{20}$ ribbons applying a constant force and a constant heating rate of 2 K min^{-1}. X-ray Photon Correlation Spectroscopy (XPCS) was performed on $Mg_{65}Cu_{25}Y_{10}$ and $Pd_{43}Ni_{10}Cu_{27}P_{20}$; the experimental details are described in the corresponding refs. [19,20].

Although following different thermal protocols, all the results presented here correspond to ribbons that were previously annealed above the glass transition temperature, thereby dramatically reducing the effect of *in situ* physical aging during the probes. Therefore, we will consider that the effect of aging is small and that the results give us insight into the temperature dependence of the α-relaxation times of isoconfigurational glassy states. All the experimental results, except the stress relaxation tests of $Pd_{42.5}Ni_{7.5}Cu_{30}P_{20}$, were already reported in previous works [19–25]. These works were devoted to the study of physical aging, and the results of the aged samples were presented together with those corresponding to as-quenched states and partially aged samples. The discussion of the change of relaxation dynamics during the aging process can be found there. Here we will compare the different systems and focus on the isoconfigurational relaxation dynamics which is not discussed in the previous works.

Results

The range of frequencies in conventional DMA experiments permits the full characterization of the α-peak above T_g, but it only determines the high-frequency side of the peak in the out-of-equilibrium region below T_g. However, in systems where the β-process is not present, or exhibits low intensity, the assumption of a constant peak shape and the application of the time-temperature-superposition (TTS) principle permits the estimation of $\tau_\alpha(T)$. In $Mg_{65}Cu_{25}Y_{10}$ and $Zr_{46}Cu_{46}Al_8$ glasses the DMA signal was interpreted in this way and the fitting of an empirical Cole-Cole (CC) function gave an estimation of $\tau_\alpha(T)$ below T_g as detailed in refs. [21,24]. As only the high-frequency side of the relaxation function is observed below T_g, using a more realistic asymmetric Havriliak-Negami (HN) function [26] does not significantly affect the estimation of $\tau_\alpha(T)$ while adding an extra fitting parameter along with the corresponding uncertainty.

Contrary to the cases of $Mg_{65}Cu_{25}Y_{10}$ and $Zr_{46}Cu_{46}Al_8$, mechanical spectroscopy of Pd-based glasses showed a prominent shoulder, manifesting the presence of a secondary relaxation. In this case, the average relaxation times $\tau_\alpha(T)$ and $\tau_\beta(T)$ as a function of temperature were estimated by considering two relaxation events combined with viscosity measurements as detailed in ref. [25]. Figure 1 shows the normalized loss modulus $M''(\omega,T)$ measured in DMA isochronal tests at $\omega/2\pi = 1\text{Hz}$ (open circles) and the $\tau_\alpha(T)$ obtained from DMA tests at different frequencies (full circles).

Isothermal static stress relaxation tests give direct access to the macroscopic response in the time domain. As discussed in ref. [4], the stress relaxation can be fitted by a stretched exponential decay, $\sigma(t) = \sigma_0 \exp\left(-(t/\tau_\alpha)^{\beta_{KWW}}\right)$, thus obtaining the average relaxation time τ_α

and the stretching exponent β_{KWW}. Figure 2 shows the stress evolution of $Zr_{46}Cu_{46}Al_8$ and $Pd_{42.5}Ni_{7.5}Cu_{30}P_{20}$ at different temperatures and the corresponding fitted stretched exponential functions. The $\tau_\alpha(T)$ values obtained from the fittings are displayed in Figure 1 as square symbols. In the case of $Mg_{65}Cu_{25}Y_{10}$ and $Pd_{43}Ni_{10}Cu_{27}P_{20}$, XPCS measurements gave direct access to the microscopic relaxation dynamics in the time domain by monitoring the decay of the autocorrelation function of the atomic positions under isothermal conditions as detailed in refs. [19,20]. The values of $\tau_\alpha(T)$ obtained by this method are reproduced from those references as diamonds in Figure 1.

Figure 1 also shows a theoretical estimation of $\tau_\alpha(T)$ (dashed lines) and loss modulus $M''(\omega,T)$ (solid lines). This estimation of $\tau_\alpha(T)$ was calculated considering that at T_g the temperature dependence of the relaxation dynamics evolves from Vogel-Fulcher-Tamman (VFT), $\tau_\alpha(T)=\tau_0\exp(B/(T-T_0))$ in the equilibrium liquid, to Arrhenius behavior, $\tau_\alpha(T)=\tau_0\exp(E_\alpha/RT)$ in the non-equilibrium glass [27,28]. The parameters used for this calculation are taken from previous analyses [21,24,25] and are specified in Table 1. The corresponding theoretical estimation of the loss modulus was calculated assuming a Havriliak-Negami (HN) relaxation function [26], $M(\omega,T)/M_0=1-\left(1+(i\omega\tau_\alpha(T))^a\right)^{-b}$ where exponents *a* and *b* are the parameters that determine the shape of the loss modulus peak. The low frequency side of the peak, $\omega\tau<<1$, follows $M''(\omega\tau)\propto(\omega\tau)^a$, while the high frequency side, $\omega\tau>>1$, decays as $M''(\omega\tau)\propto(\omega\tau)^{-ab}$. Therefore, the high frequency side exponent can be obtained from the data as the slope of a $\log(M'')$ vs $\log(\omega)$ plot, obtaining average values of ab=0.35, 0.40, 0.33 for $Zr_{46}Cu_{46}Al_8$, $Mg_{65}Cu_{25}Y_{10}$ and $Pd_{42.5}Ni_{7.5}Cu_{30}P_{20}$ respectively. These values are used for plotting the solid line in figure 2.

Discussion

This work is focused on the behavior of $\tau_\alpha(T)$ below T_g, compiling new and literature data from metallic glasses having varying fragility parameters (see Table 1) and obtained by different experimental techniques; Figure 3 shows all the experimental $\tau_\alpha(T)$ values as a function of T_g/T. At the glass transition, all systems show the expected change from liquid to isoconfigurational glass with the corresponding decrease in the slope of the log(τ_α) vs T_g/T plot upon entering the sub-T_g region. The first point to be discussed is the common behavior observed in Figure 3 in the region from T_g/T=1 to T_g/T=1.1, with relaxation times showing an activation energy roughly described by an overall $E_\alpha \approx 40RT_g$ rule. Similar normalized activation energy values are also found in the literature for other metallic glasses [27]. Figure 3 shows that the differences in apparent activation energy above T_g, where it is found that $E_\alpha^{liq}/RT_g = 90-160$ which reflects the fragility parameter, become mostly mitigated when entering the glassy regime where $E_\alpha/RT_g = 30-50$ in all three glassy materials. Considering that the T_g of metallic glasses is directly proportional to their elastic constants and, therefore, to the strength of their interatomic bonding [16], these results suggest that the activation of the atomic-level movements involved in both the α and β processes is basically dependent on the interatomic bonding strength, while involving a similar number of atoms in all metallic glasses. The values of E_α^{liq}/E_α are in reasonable agreement with the ratio between the apparent equilibrium and non-equilibrium activation energies estimated for liquids with fragility parameter $m = 40-70$ by the random first-order transition theory [29].

In the lower temperature region, T_g/T>1.1, the relaxation times become longer than 10^4 s. This implies that the $\tau_\alpha(T)$ obtained from DMA correspond to the fitting of just the very high-frequency tail of the loss modulus [24] and that the static measurements only cover the initial steps of the stress relaxation. In the case of the DMA measurements this implies that the shape of the relaxation function cannot be well assessed from the experimental data. Therefore, the relaxation times are obtained assuming the same functional shape observed in the sub-T_g and supercooled liquid regions. In the case of the static stress relaxation experiments, the quality of the fitting with a single stretched exponential decay is also poor, because the relaxation starts to decouple in two relaxation time scales as will be discussed below. Hence, the overall relaxation times obtained in this T_g/T>1.1 region have to be taken with precaution. In this temperature region the $Pd_{42.5}Ni_{7.5}Cu_{30}P_{20}$ system shows an important reduction of the activation energy while the $Zr_{46}Cu_{46}Al_8$ glass does not. It has been established that the relaxation behavior of metallic glasses at and around T_g is intimately linked to their fragilities [30,31]. Whether this almost constant behavior of τ_α vs temperature of the Pd-based glass is related to its fragility, the presence of a significant β process or the de-coupling of different relaxation mechanisms cannot be assessed without further evidence.

While the overall relaxation time in both the liquid and glassy states is well described by VFT and Arrhenius laws in the T_g/T=0.9-1.1 region, showing agreement between the different materials and experimental techniques, the inspection of other features characterizing the relaxation process shows significant differences. Particularly, it is interesting to discuss here the behavior of the broadening parameter, β_{KWW}, available from DMA, static stress relaxation and XPCS experiments. In DMA, β_{KWW} is obtained indirectly

as the slope of the high frequency wing of the loss peak in a log-log plot [32]. Figure 4 shows the values of β_{KWW} obtained by the different techniques. From DMA and stress relaxation tests, β_{KWW} is always lower than one with an approximate constant value at low temperatures and an increase at temperatures near or above the glass transition [33]. This is in agreement with other mechanical investigations [4] and with works considering other macroscopic quantities (e.g. volume, enthalpy) [34]. More recent results [35] show that the increase of β_{KWW} near T_g of $Cu_{46}Zr_{46}Al_8$ is less evident if the analysis is performed over a DMA response extended in a wider frequency and temperature ranges, but the overall values in the sub-T_g region are similar to the ones presented here. Furthermore, while near the glass transition a single stretched exponential is able to characterize the stress decay of the static relaxation probes, at temperatures $T_g/T>1.1$ the temporal response cannot be well described by a single stretched exponential (see Figure 2 bottom). In refs. [36] and [37] the stress relaxation curves of several metallic glasses were shown to be composed of two regimes, an initial stress decay assigned to a stress-driven process [36] and a slower stress decay with a thermally activated relaxation time. The two relaxation time scales decouple as temperature decreases [37].

In XPCS experiments, the results show an evolution of β_{KWW} from stretched ($\beta_{KWW}<1$) to compressed ($\beta_{KWW}>1$) on lowering the temperature below T_g. This behavior was found to be an indicator of a change from diffusional-like atomic-scale dynamics in the liquid to stress-driven ballistic motion in the glass [19,20]. The crossover between the two different motions occurs at the same temperature where the structural relaxation time deviates from the liquid behavior. In agreement with Figure 3, this crossover occurs sooner in the Pd-based MG. The underlying difference between macroscopic stress relaxation (β_{KWW}=0.3-

0.7) and microscopic glassy dynamics (β_{KWW}>1) could be related to different aspects as the anelastic contribution existing in the macroscopic response; this anelastic contribution is not present in the XPCS studies as they are carried out without the application of an external force. In spite of the fast anelastic contribution, which clearly influences the shape of the macroscopic stress decay, the overall coincidence of all $\tau_\alpha(T)$ measurements – irrespective of experimental probe – indicates that the remaining macroscopic stress decay involves the same microscopic movements responsible for the atomic-level dynamics unveiled by XPCS. It should be noted here that β_{KWW}>1, as determined in XPCS studies, represents a unique form of the relaxation function, which is not currently accounted for in any current theories of aging and the glass transition. In addition, in all cases β_{KWW} is basically temperature independent in the glassy state, in contrast to theoretical studies that predict a systemic decrease of β_{KWW} as the temperature is lowered [29]. These two points above should be taken into account when critically evaluating any contemporary theory of the glass transition as it relates to metallic glasses.

The last point of this discussion is the implications of this study for the current models and descriptions of α and β processes in metallic glasses. The activation energy of the α relaxation has been evaluated in the equilibrium super-cooled liquid in many works, giving values of $E_\alpha^{liq}/RT_g = 90-160$ compared to $E_\beta/RT_g \approx 26$ as discussed above. However, from the results compiled here, in an isoconfigurational glassy state the ratio between the activation energies of both processes appears to be $E_\alpha/E_\beta = 1-2$, in contrast to a $E_\alpha^{liq}/E_\beta = 3-6$. If the apparent activation energies are proportional to the number of correlated atoms involved in the relaxation processes, as suggested in some works [38], the

results presented here should be taken into account when debating the microscopic descriptions of α and β processes in metallic glasses. We note here that each particular isoconfigurational state may have a different activation energy. However, while a relatively small change of fictive temperature produces an important change of magnitude of τ_α, the dependence of $E_\alpha(T_f)$ is not expected to be strong [24][27].

Another important aspect in this point concerns the modeling of the loss modulus shown in Figure 1 (solid line), which reproduces the overall behavior shown by $Zr_{46}Cu_{46}Al_8$ and $Mg_{65}Cu_{25}Y_{10}$ glasses without the necessity of introducing a separate, secondary β process. In these two glasses it seems that the fastest movements of the mechanical relaxation spectrum, considered as the precursors of the α (viscous-like) relaxation, are comprised within the broad high-frequency wing of the α-peak. We observe no direct evidence of a separate, fast relaxation process in these systems. On the contrary, in the Pd-based material these fastest processes are well differentiated from the main relaxation peak [25], similar to other metallic glass systems such the La-based family [39]. The presence or absence of secondary relaxation processes well differentiated from the main structural relaxation in the frequency-temperature window explored by mechanical spectroscopy is also an important point to consider when constructing an overall PEL picture of metallic glasses [4]. It is worth to stress here that $\tau_\alpha(T)$ is the average relaxation time of a broad relaxation spectrum, which comprises different microscopic processes and activation energies more or less coupled depending on the temperature. Detailed studies of the relaxation spectrum, such as the direct spectrum analysis [40,41], will help to unveil the detailed temperature behavior and the contribution of the different microscopic processes and time scales involved in metallic glass relaxation dynamics.

Conclusions

Experimental data of α relaxation times of $Zr_{46}Cu_{46}Al_8$, $Mg_{65}Cu_{25}Y_{10}$, $Pd_{42.5}Ni_{7.5}Cu_{30}P_{20}$ and $Pd_{43}Ni_{10}Cu_{27}P_{20}$ glasses were collected by different macroscopic and microscopic techniques. These three systems comprise very different fragility and T_g. When rescaled by the glass transition temperature, all the systems show a common temperature behavior in the $0.9T_g$-T_g region. The activation energy of the α relaxation in this temperature range is roughly twice of that what is expected for the faster β process. For the $Pd_{42.5}Ni_{7.5}Cu_{30}P_{20}$ glass, an important reduction in activation energy is noticed at even lower temperatures. Whether this is a result of a more pronounced β process, or a higher fragility, is currently under investigation. The macroscopic response monitored by stress relaxation tests and the microscopic insight given by XPCS experiments coincide with the average $\tau_\alpha(T)$ values, although they completely and fundamentally differ in the relaxation function shape. These differences can be attributed in part to the anelastic contribution present in the macroscopic response or to an intrinsic property of the probed length scale, suggesting a unique, length scale-dominated dynamics. More experimental determinations of α relaxation below T_g, both by XPCS and macroscopic techniques will refine the general picture of isoconfigurational relaxation dynamics presented in this work.

Tables

	m	T_g (K)	τ_0 (s)	B (K)	T_0 (K)	E_α (kJ mol^{-1})
$Zr_{46}Cu_{46}Al_8$,	57-63 (refs. [24,42])	694	6.0×10^{-13}	6220	512	197
$Mg_{65}Cu_{25}Y_{10}$	39-45 (refs. [5,21,43])	412	2.4×10^{-15}	5750	260	129
$Pd_{42.5}Ni_{7.5}Cu_{30}P_{20}$ / $Pd_{43}Ni_{10}Cu_{27}P_{20}$	65-75 (refs. [25,44–46])	560	8.2×10^{-14}	4400	436	230

Table 1. Experimental fragility parameter of the glassy alloys studied in this work, taken from the specified references. Glass transition temperature T_g, VFT parameters τ_0, B and T_0 and Arrhenius activation energy E_α, used for depicting the $\tau_\alpha(T)$ behavior (dashed lines in Figure 1).

Figure Captions

Figure 1. Normalized loss modulus $M''(\omega, T)$ at $\omega/2\pi$=1Hz; DMA measurements (open circles) and theoretical calculation considering an HN model and $\tau_\alpha(T)$ with VFT+Arrhenius behavior given by the parameters in Table 1 (continuous line). Relaxation times as a function of temperature; Static stress relaxation tests (squares), DMA measurements applying TTS principle (full circles), XPCS experiments (diamonds) and elongation viscosity (open triangles). Dashed lines correspond to $\tau_\alpha(T)$ with VFT+Arrhenius behavior given by the parameters in Table 1.

Figure 2. Stress evolution during isothermal static stress relaxation tests; experimental values (symbols) and fitted stretched exponential functions (lines). Top: $Zr_{46}Cu_{46}Al_8$ at 633 K, 653 K, 663 K, 673 K, 683 K and 693 K. Middle: $Pd_{42.5}Ni_{7.5}Cu_{30}P_{20}$ at 453 K, 533 K, 543 K, 553 K, 563 K and 573 K. Bottom: Semi-log plots of stress relaxation tests of $Pd_{42.5}Ni_{7.5}Cu_{30}P_{20}$ at 513 K and 553 K (Left) and $Zr_{46}Cu_{46}Al_8$ at 633 K and 693 K (Right).

Figure 3. Experimental values of $\tau_\alpha(T)$. Static stress relaxation tests of $Zr_{46}Cu_{46}Al_8$ [24] (red squares) and $Pd_{42.5}Ni_{7.5}Cu_{30}P_{20}$ [this work] (green squares); DMA measurements applying TTS principle of $Zr_{46}Cu_{46}Al_8$ [24] (orange full circles) and $Mg_{65}Cu_{25}Y_{10}$ [21] (blue full circles); XPCS experiments of $Mg_{65}Cu_{25}Y_{10}$ [19] (blue diamonds) and $Pd_{43}Ni_{10}Cu_{27}P_{20}$ [20] (green diamonds); Elongation viscosity of $Pd_{42.5}Ni_{7.5}Cu_{30}P_{20}$ [25] (green open triangles). Dashed lines are guides to the eyes showing the temperature behaviors expected for α and β relaxations with activation energies of $E_\alpha=40RT_g$ and $E_\beta=26RT_g$.

Figure 4. Stretching exponents of the relaxation response. Static stress relaxation tests of $Zr_{46}Cu_{46}Al_8$ [24] (red squares) and $Pd_{42.5}Ni_{7.5}Cu_{30}P_{20}$ [this work] (green squares); DMA measurements of $Zr_{46}Cu_{46}Al_8$ [24] (orange full circles) and $Mg_{65}Cu_{25}Y_{10}$ [21] (blue full circles); XPCS experiments of $Mg_{65}Cu_{25}Y_{10}$ [19] (blue diamonds) and $Pd_{43}Ni_{10}Cu_{27}P_{20}$ [20] (green diamonds).

Acknowledgments

C. Liu thanks the experimental assistance and the fruitful discussions with Mr. M. Madinehei and Dr. P. Bruna. Work funded by MINECO, grant FIS2014-54734-P, and Generalitat de Catalunya, grant 2014SGR00581. C. Liu is supported by Generalitat de Catalunya, FI grant 2012FI_B00237. J.C. Qiao is supported by the National Natural Science Foundation of China (Grant No. 51401192) and the Natural Science Foundation of Shaanxi Province (Grant No. 2016JM5009).

References

[1] P. Lunkenheimer, U. Schneider, R. Brand, A. Loid, Glassy dynamics, Contemp. Phys. 41 (2000) 15–36. doi:10.1080/001075100181259.

[2] H.-B. Yu, W.-H. Wang, K. Samwer, The beta relaxation in metallic glasses: an overview, Mater. Today. 16 (2013) 183–191. doi:10.1016/j.mattod.2013.05.002.

[3] H. Bin Yu, W.H. Wang, H.Y. Bai, K. Samwer, The β-relaxation in metallic glasses, Natl. Sci. Rev. 1 (2014) 429–461. doi:10.1093/nsr/nwu018.

[4] Z. Wang, B.A. Sun, H.Y. Bai, W.H. Wang, Evolution of hidden localized flow during glass-to-liquid transition in metallic glass., Nat. Commun. 5 (2014) 5823. doi:10.1038/ncomms6823.

[5] R. Busch, W. Liu, W.L. Johnson, Thermodynamics and kinetics of the Mg65Cu25Y10 bulk metallic glass forming liquid, J. Appl. Phys. 83 (1998) 4134–4141. doi:10.1063/1.367167.

[6] J. Qiao, J.-M. Pelletier, R. Casalini, Relaxation of bulk metallic glasses studied by mechanical spectroscopy., J. Phys. Chem. B. 117 (2013) 13658–66. doi:10.1021/jp4067179.

[7] J.C. Qiao, J.M. Pelletier, Dynamic Mechanical Relaxation in Bulk Metallic Glasses: A Review, J. Mater. Sci. Technol. 30 (2014) 523–545. doi:10.1016/j.jmst.2014.04.018.

[8] R. Böhmer, K.L. Ngai, C.A. Angell, D.J. Plazek, Nonexponential relaxations in strong and fragile glass formers, J. Chem. Phys. 99 (1993) 4201–4209. doi:10.1063/1.466117.

[9] J.J. Lewandowski, W.H. Wang, A.L. Greer, Intrinsic plasticity or brittleness of metallic glasses, Philos. Mag. Lett. 85 (2005) 77–87. doi:10.1080/09500830500080474.

[10] P. Murali, U. Ramamurty, Embrittlement of a bulk metallic glass due to sub-Tg annealing, Acta Mater. 53 (2005) 1467–1478. doi:10.1016/j.actamat.2004.11.040.

[11] Y. Zhang, W.H. Wang, A.L. Greer, Making metallic glasses plastic by control of residual stress, Nat. Mater. 5 (2006) 857–860. doi:10.1038/nmat1758.

[12] Y. Tong, W. Dmowski, Y. Yokoyama, G. Wang, P.K. Liaw, T. Egami, Recovering compressive plasticity of bulk metallic glasses by high-temperature creep, Scr. Mater. 69 (2013) 570–573. doi:10.1016/j.scriptamat.2013.06.020.

[13] C.T. Moynihan, A.J. Easteal, M.A. Bolt, J. Tucker, Dependence of the Fictive Temperature of Glass on Cooling Rate, J. Am. Ceram. Soc. 59 (1976) 12–16. doi:10.1111/j.1151-2916.1976.tb09376.x.

[14] L. Hu, Y. Yue, Secondary Relaxation in Metallic Glass Formers: Its Correlation with the Genuine Johari-Goldstein Relaxation, J. Phys. Chem. C. 113 (2009) 15001–15006. doi:10.1021/jp903777f.

[15] Z. Wang, H.B. Yu, P. Wen, H.Y. Bai, W.H. Wang, Pronounced slow beta-relaxation in La-based bulk metallic glasses, J. Phys. Condens. Matter. 23 (2011) 142202.

doi:10.1088/0953-8984/23/14/142202.

[16] W.H. Wang, Correlation between relaxations and plastic deformation, and elastic model of flow in metallic glasses and glass-forming liquids, J. Appl. Phys. 110 (2011) 53521. doi:10.1063/1.3632972.

[17] V.M. Giordano, B. Ruta, Unveiling the structural arrangements responsible for the atomic dynamics in metallic glasses during physical aging, Nat. Commun. 7 (2016) 10344. doi:10.1038/ncomms10344.

[18] A. Heuer, Exploring the potential energy landscape of glass-forming systems: from inherent structures via metabasins to macroscopic transport., J. Phys. Condens. Matter. 20 (2008) 373101. doi:10.1088/0953-8984/20/37/373101.

[19] B. Ruta, Y. Chushkin, G. Monaco, L. Cipelletti, E. Pineda, P. Bruna, V.M. Giordano, M. Gonzalez-Silveira, Atomic-Scale Relaxation Dynamics and Aging in a Metallic Glass Probed by X-Ray Photon Correlation Spectroscopy, Phys. Rev. Lett. 109 (2012) 165701. doi:10.1103/PhysRevLett.109.165701.

[20] Z. Evenson, B. Ruta, S. Hechler, M. Stolpe, E. Pineda, I. Gallino, R. Busch, X-Ray Photon Correlation Spectroscopy Reveals Intermittent Aging Dynamics in a Metallic Glass, Phys. Rev. Lett. 115 (2015) 175701. doi:10.1103/PhysRevLett.115.175701.

[21] E. Pineda, P. Bruna, B. Ruta, M. Gonzalez-Silveira, D. Crespo, Relaxation of rapidly quenched metallic glasses: Effect of the relaxation state on the slow low temperature dynamics, Acta Mater. 61 (2013) 3002–3011. doi:10.1016/j.actamat.2013.01.060.

[22] B. Ruta, V.M. Giordano, L. Erra, C. Liu, E. Pineda, Structural and dynamical properties of Mg65Cu25Y10 metallic glasses studied by in situ high energy X-ray diffraction and time resolved X-ray photon correlation spectroscopy, J. Alloys Compd. 615 (2013) S45–S50. doi:10.1016/j.jallcom.2013.12.162.

[23] F. Zhai, E. Pineda, B. Ruta, M. Gonzalez-Silveira, D. Crespo, Aging and structural relaxation of hyper-quenched Mg65Cu25Y10 metallic glass, J. Alloys Compd. 615 (2013) S9–S12. doi:10.1016/j.jallcom.2013.11.120.

[24] C. Liu, E. Pineda, D. Crespo, Characterization of mechanical relaxation in a Cu–Zr–Al metallic glass, J. Alloys Compd. 643 (2015) S17–S21. doi:10.1016/j.jallcom.2014.10.101.

[25] C. Liu, E. Pineda, J. Qiao, D. Crespo, Modeling of the Sub-Tg Relaxation Spectrum of Pd42.5Ni7.5Cu30P20 Metallic Glass., J. Phys. Chem. B. 120 (2016) 2838–44. doi:10.1021/acs.jpcb.5b11754.

[26] S. Havriliak, S. Negami, A complex plane representation of dielectric and mechanical relaxation processes in some polymers, Polymer (Guildf). 8 (1967) 161–210. doi:10.1016/0032-3861(67)90021-3.

[27] A.I. Taub, F. Spaepen, THE KINETICS OF STRUCTURAL RELAXATION OF A METALLIC-GLASS, ACTA Metall. 28 (1980) 1781–1788. doi:10.1016/0001-6160(80)90031-0.

[28] I.M. Hodge, Effects of Annealing and Prior History on Enthalpy Relaxation in Glassy-Polymers .6. Adam-Gibbs Formulation of Nonlinearity, Macromolecules. 20 (1987) 2897–2908. doi:10.1021/ma00177a044.

[29] V. Lubchenko, P.G. Wolynes, Theory of aging in structural glasses., J. Chem. Phys. 121 (2004) 2852–65. doi:10.1063/1.1771633.

[30] S. Wei, Z. Evenson, I. Gallino, R. Busch, The impact of fragility on the calorimetric glass transition in bulk metallic glasses, Intermetallics. 55 (2014) 138–144. doi:10.1016/j.intermet.2014.07.018.

[31] S. Wei, M. Stolpe, O. Gross, Z. Evenson, I. Gallino, W. Hembree, J. Bednarcik, J.J. Kruzic, R. Busch, Linking structure to fragility in bulk metallic glass-forming liquids, Appl. Phys. Lett. 106 (2015) 181901. doi:10.1063/1.4919590.

[32] C. Svanberg, Correlation function for relaxations in disordered materials, J. Appl. Phys. 94 (2003) 4191–4197. doi:10.1063/1.1601295.

[33] C. Liu, Dynamics of metallic glasses explored by mechanical relaxation, Universitat Politècnica Catalunya - BarcelonaTech, 2015.

[34] Z. Evenson, R. Busch, Equilibrium viscosity, enthalpy recovery and free volume relaxation in a Zr44Ti11Ni10Cu10Be25 bulk metallic glass, Acta Mater. 59 (2011) 4404–4415. doi:10.1016/j.actamat.2011.03.064.

[35] J. Qiao, To be published, To Be Publ. (n.d.).

[36] J.C. Qiao, Y.-J. Wang, L.Z. Zhao, L.H. Dai, D. Crespo, J.M. Pelletier, L.M. Keer, Y. Yao, Transition from stress-driven to thermally activated stress relaxation in metallic glasses, Phys. Rev. B. 94 (2016) 104203. doi:10.1103/PhysRevB.94.104203.

[37] P. Luo, P. Wen, H.Y. Bai, B. Ruta, W.H. Wang, Relaxation Decoupling in Metallic Glasses at Low Temperatures, Phys. Rev. Lett. 118 (2017) 225901. doi:10.1103/PhysRevLett.118.225901.

[38] T. Bauer, P. Lunkenheimer, S. Kastner, A. Loidl, Nonlinear Dielectric Response at the Excess Wing of Glass-Forming Liquids, Phys. Rev. Lett. 110 (2013) 107603. doi:10.1103/PhysRevLett.110.107603.

[39] C. Liu, E. Pineda, D. Crespo, Mechanical Relaxation of Metallic Glasses: An Overview of Experimental Data and Theoretical Models, Metals (Basel). 5 (2015) 1073–1111. doi:10.3390/met5021073.

[40] J.D. Ju, D. Jang, A. Nwankpa, M. Atzmon, An atomically quantized hierarchy of shear transformation zones in a metallic glass, J. Appl. Phys. 109 (2011) 53522. doi:10.1063/1.3552300.

[41] J.D. Ju, M. Atzmon, A comprehensive atomistic analysis of the experimental dynamic-mechanical response of a metallic glass, Acta Mater. 74 (2014) 183–188. doi:10.1016/j.actamat.2014.04.012.

[42] S. Pauly, J. Das, N. Mattern, D.H. Kim, J. Eckert, Phase formation and thermal stability in Cu-Zr-Ti(Al) metallic glasses, Intermetallics. 17 (2009) 453–462. doi:10.1016/j.intermet.2008.12.003.

[43] D.N. Perera, Compilation of the fragility parameters for several glass-forming metallic alloys, J. Phys. Condens. Matter. 11 (1999) 3807–3812. doi:10.1088/0953-8984/11/19/303.

[44] G.J. Fan, H.-J. Fecht, E.J. Lavernia, Viscous flow of the Pd43Ni10Cu27P20 bulk

metallic glass-forming liquid, Appl. Phys. Lett. 84 (2004) 487. doi:10.1063/1.1644052.

[45] I. Gallino, J. Schroers, R. Busch, Kinetic and thermodynamic studies of the fragility of bulk metallic glass forming liquids, J. Appl. Phys. 108 (2010) 63501. doi:10.1063/1.3480805.

[46] J. Qiao, R. Casalini, J.-M. Pelletier, H. Kato, Characteristics of the structural and Johari-Goldstein relaxations in Pd-based metallic glass-forming liquids., J. Phys. Chem. B. 118 (2014) 3720–30. doi:10.1021/jp4121782.

Figure 1

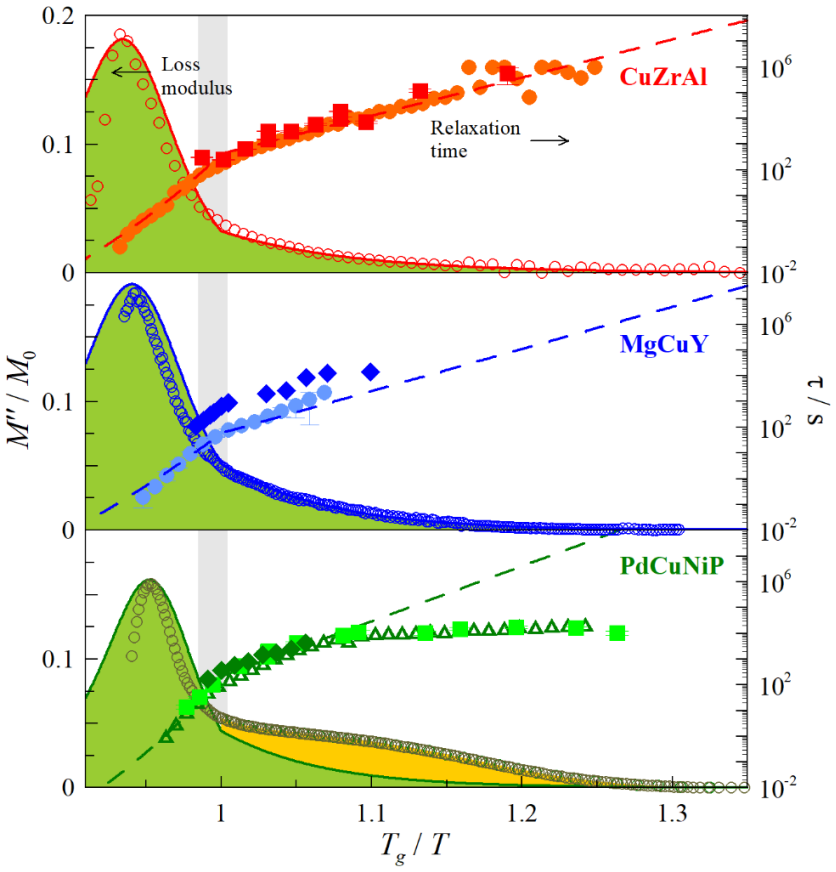

Figure 1.

Figure 2

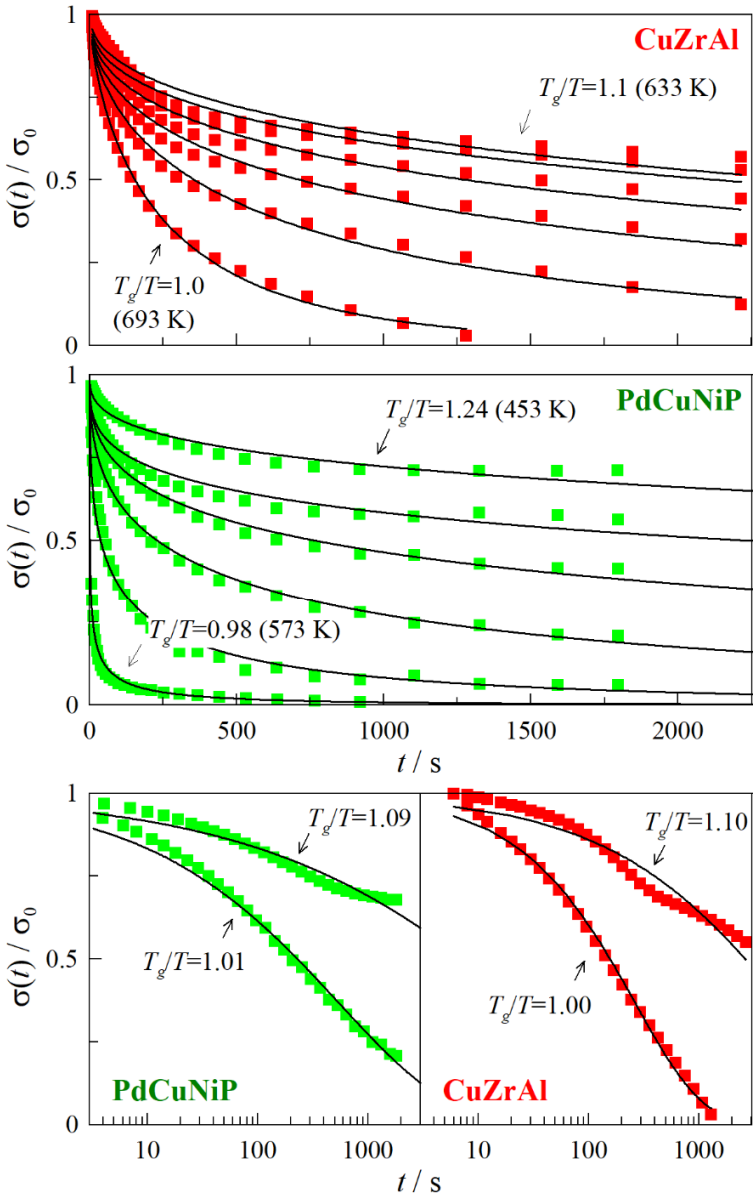

Figure 2.

Figure 3

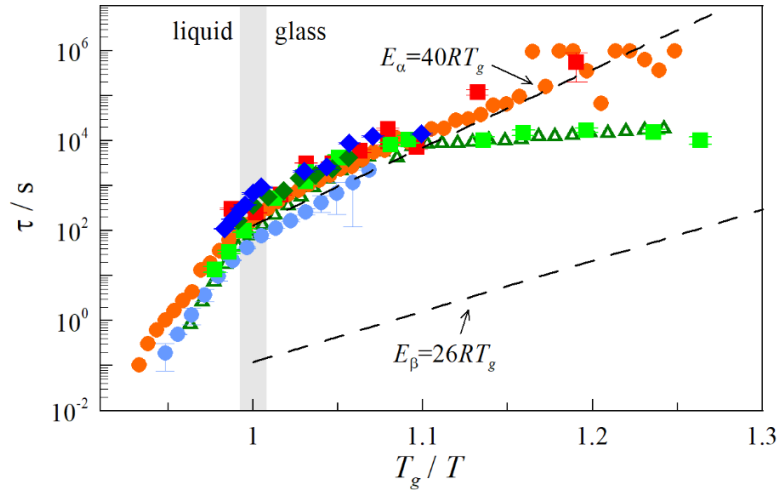

Figure 3.

Figure 4

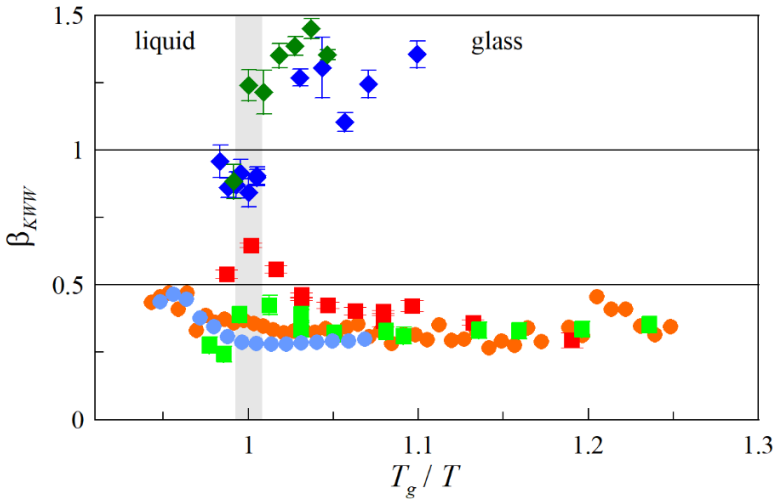

Figure 4.